RuO$_2$ supported on V$_2$O$_5$–Al$_2$O$_3$ material as heterogeneous catalyst for cyclohexane oxidation reaction

YASMINA NESRINE TCHENAR, ABDERRAHIM CHOUKCHOU-BRAHAM[*] **and REDOUANE BACHIR**

Laboratoire de catalyse et synthèse en chimie organique, Faculté des sciences. Université A. Belkaid Tlemcen, BP 119 Tlemcen 13000 Algérie

Abstract. **RuO$_2$ supported on V$_2$O$_5$–Al$_2$O$_3$ mixed oxide material was prepared by impregnation method and characterized by XRD, nitrogen adsorption–desorption, SEM, UV-visible and FT–IR spectroscopic techniques. The catalytic activity of the prepared catalyst was evaluated for the liquid-phase oxidation of cyclohexane under mild conditions. In this reaction, conversion of cyclohexane to cyclohexanol and cyclohexanone and the selectivity ratio of cyclohexanol to cyclohexanone were greatly affected by the solvent and the oxidant agent used. The results show that the catalyst exhibit good conversion in polar solvents. The use of acetic acid gives more than 26% conversion in presence of TBHP as oxidant and an ~40% conversion with hydrogen peroxide as oxidant in presence of an initiator, with 92% selectivity for cyclohexanol product.**

Keywords. **Ruthenium oxide; sol–gel method; impregnation; cyclohexane oxidation.**

1. Introduction

The present-day interest in the chemistry of ruthenium dioxide, RuO$_2$, is primarily due to the existing or possible applications of the material in advanced technologies. It is an attractive metallic oxide for electrochemical, catalytic and electronic applications (Nada *et al* 2008; Yu *et al* 2009; Patake *et al* 2010; Wong *et al* 2010). The chemistry of RuO$_2$ is more complex than that of many other metal oxides. The reason is very simple, ruthenium easily changes the oxidation numbers in dependence on the experimental conditions (Rard 1985).

The role of ruthenium oxide-based catalysts in oxidation reactions was confirmed, for example, the oxidation of cinnamyl alcohol on Ru–Co mixed oxide (Stuchinskaya *et al* 2005), of benzyl alcohol on hydrous ruthenium (IV) dioxide nanoparticles supported by carbon nanotubes (RuO$_2$· xH$_2$O/CNT) (Yu *et al* 2009), of 2-octanol on Ru/Mn/Ce mixed oxide (Chęciński *et al* 2009), and of cyclohexene on Ru/Co/Ce mixed oxide (Ghiaci *et al* 2011).

Cyclohexane oxidation has also been the subject of a variety of studies and is still a challenging and promising reaction from academic and industrial points view (Aboelfetoh and Pietschnig 2009; Mahmudov *et al* 2010). As an important commercial reaction (Schuchardt *et al* 2001), the cyclohexane oxidation process produces cyclohexanol and cyclohexanone, which are important intermediates in the petrochemical industry. They are used principally for the production of adipic acid and caprolactam, which are key materials for manufacturing nylon-6,6 and nylon-6, respectively.

In this work, we propose synthesis and characterization of 5 wt% RuO$_2$ supported on V$_2$O$_5$–Al$_2$O$_3$ mixed oxide, as well as the evaluation of its catalytic activity in the oxidation of cyclohexane using hydrogen peroxide or tert-butyl hydroperoxide as oxidant.

2. Experimental

2.1 *Starting materials*

The following chemicals were employed for the preparation of V$_2$O$_5$–Al$_2$O$_3$ support: vanadium oxide (V$_2$O$_5$; sigma), aluminum iso-propoxide (Al(OC$_3$H$_7$)$_3$; Aldrich, 98%), butanol (Aldrich), hydrogen peroxide (H$_2$O$_2$; Prolabo, 30% in water) and acetic acid (Prolabo, 99–100%). For the RuO$_2$/V$_2$O$_5$–Al$_2$O$_3$ synthesis, we used the ruthenium acetyl acetonate (Ru(C$_5$H$_7$O$_2$)$_3$; Aldrich, 97%) and acetone (Prolabo; 99%).

Cyclohexane (Prolabo; 98%), cyclohexanol (Merk-Schuchardt, 99%), tert-butyl hydroperoxide (TBHP; Aldrich, 70% in water), hydrogen peroxide, acetone and acetic acid were used for cyclohexane oxidation reactions.

2.2 *Sol–gel synthesis of V$_2$O$_5$–Al$_2$O$_3$ support*

The 5 wt% V$_2$O$_5$–Al$_2$O$_3$ support was synthesized by the sol–gel process (Bellifa *et al* 2006; Tchenar *et al* 2006;

Lahcene *et al* 2009). A 0·15 g of vanadium dioxide was dissolved in 20 ml of hydrogen peroxide; the resulting solution was stirred for 30 min and then a mixture containing 11·42 g of aluminum isopropoxide, 2 ml of acetic acid and 25 ml of butanol was added into solution. The obtained yellow gel was aged for 24 h at room temperature, dried at 65°C and then calcined at 300°C for 6 h (5°C/min) in air.

2.3 *Synthesis of 5 wt% RuO₂/ V₂O₅–Al₂O₃ catalyst*

The 5 wt% $RuO_2/V_2O_5–Al_2O_3$ catalyst was prepared by impregnation method. A 0·84 g of ruthenium acetyl acetonate was dissolved in 40 ml of acetone and then mixed with 5·16 g of the $V_2O_5–Al_2O_3$ support. The resulting solution was stirred for 24 h. After solvent evaporation, the impregnated product was dried at 65°C and calcined at 250°C for 6 h (5°C/min) in air.

2.4 *Characterization of materials*

The 5 wt% $V_2O_5–Al_2O_3$ and 5 wt% $RuO_2/V_2O_5–Al_2O_3$ materials were characterized by X-ray powder diffraction (XRD) using a Philips PW 3710 diffractometer with Cu Kα radiation ($\lambda = 1·54060$) in the range of $2\theta = 10–70°$ to determine the identity of any phase present.

The specific surface area, average pore volume and average pore diameter were determined from N₂ adsorption–desorption isotherm at 77 K using a Nova 1000^e (Quantachrome) instrument. Before adsorption, the sample was

degassed at 523 K for 2 h under a flow of nitrogen. The surface area was examined using a single point Brunauer–Emmett–Teller (BET) method (Brunauer *et al* 1938). The pore volume and pore diameter were calculated from the adsorption branch of the nitrogen isotherm, using the Barrett–Joyner–Halenda method (Barrett *et al* 1951).

Scanning electron microscopy (SEM) was performed on a TM-1000 HITACHI scanning electron microscope to observe the morphology of the $V_2O_5–Al_2O_3$ and $RuO_2/V_2O_5–Al_2O_3$ powders.

Ultraviolet-visible diffused reflectance (UV-vis-DR) spectra of the solids were recorded on a Perkin Elmer, Lambda 800 spectrophotometer.

The materials have also been investigated by Fourier transform infrared spectroscopy (FT–IR) using an AVATAR 320 Thermo-Nicolet FT–IR spectrometer to identify the vibration features of the functional groups in these samples.

2.5 *Catalytic cyclohexane oxidation tests*

Cyclohexane oxidation reactions were carried out in a 250 ml three-necked flask, placed in a temperature equilibrated water bath and fitted with a reflux condenser. Typically, a mixture containing 66·5 mmol cyclohexane, 66·5 mmol oxidant (H_2O_2), 24·8 ml solvent and 100 mg $RuO_2/V_2O_5–Al_2O_3$ catalyst was magnetically stirred under atmospheric pressure at 343 K for 6 h. When the TBHP was used as oxidant, a solution of tert-butyl hydroperoxide in cyclohexane
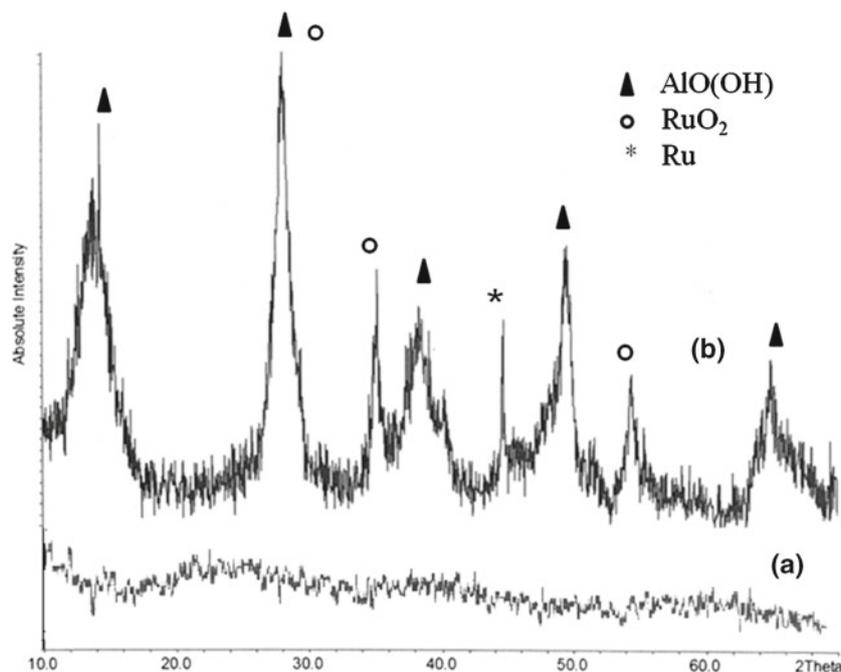

Figure 1. XRD patterns of (a) V₂O₅–Al₂O₃ and (b) RuO₂/V₂O₅–Al₂O₃ materials.

was previously prepared as follows: 66·5 mmol of cyclohexane was mixed with 66·5 mmol of TBHP in a closed Erlenmeyer flask and magnetically stirred for 24 h. The organic phase was separated from the aqueous one, put in the three-necked flask with solvent and catalyst and then heated to 343 K under vigorous agitation.

The consumption of H_2O_2 or TBHP was determined by iodometric titration (Baccam *et al* 1985) and the reaction mixture was analysed by gas chromatography (GC), taking aliquots at different reaction times. A Shimadzu GC-14 B gas chromatograph equipped with an Apiezon L column (10% on Chromosorb P UNDMCS) and a flame ionization detector (FID) was used. To such an end, 0·5 ml of sample was added to 0·04 ml of internal standard 1-pentanol (Prolabo) and 0·3 μl of this mixture was analysed.

The catalytic activities reported as conversion (%) and selectivity (%) calculated are as follows:

$$\% \text{ conversion} = \frac{\text{mmol of cyclohexanol} + \text{mmol of cyclohexanone}}{\text{mmol of starting cyclohexane}} \times 100,$$

$$\% \text{ selectivity for } X = \frac{\text{mmol of } X \text{ product}}{\text{mmol of cyclohexanol} + \text{mmol of cyclohexanone}} \times 100,$$

where X is the cyclohexanol or cyclohexanone.

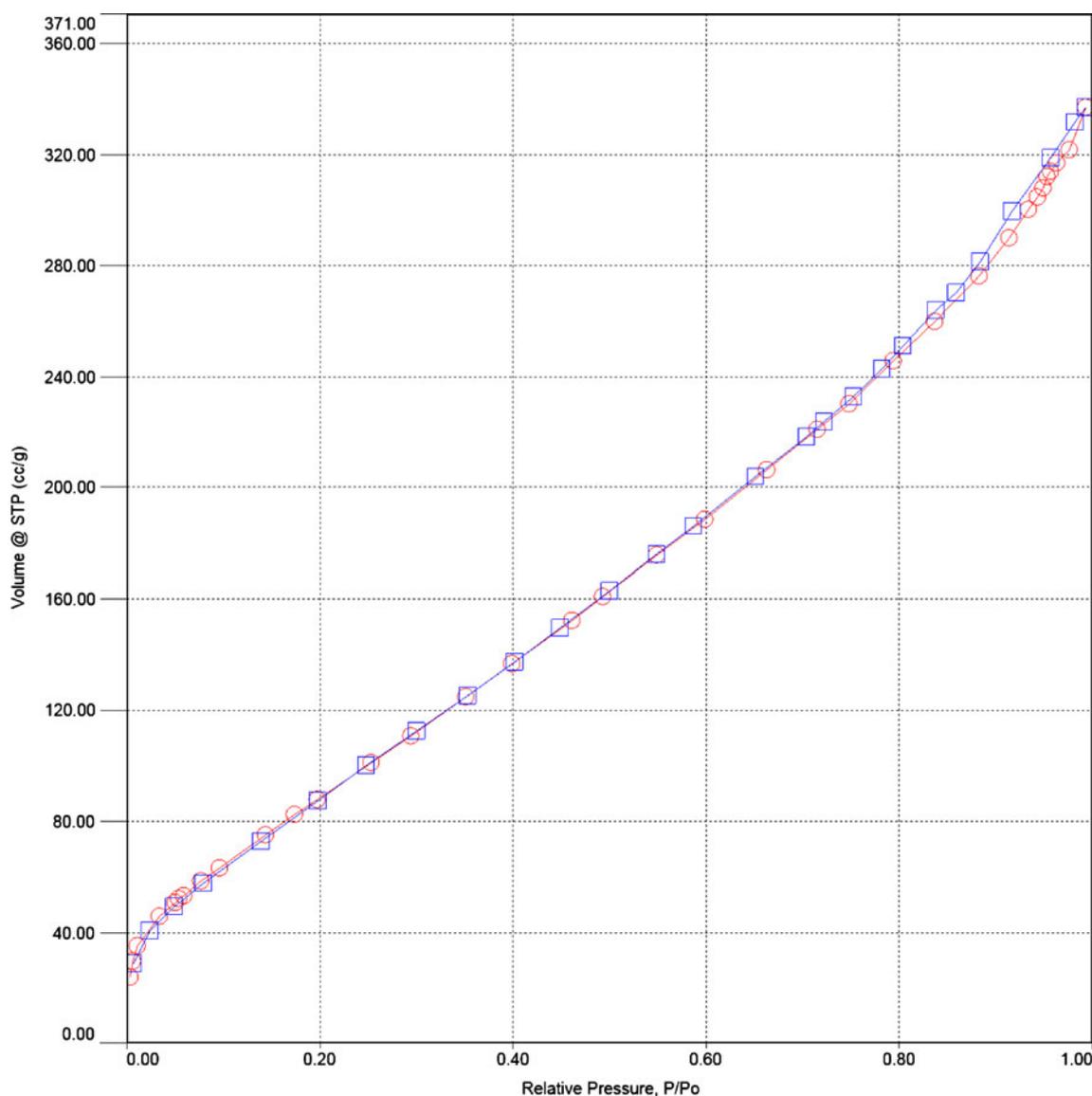**Figure 2.** Nitrogen adsorption–desorption isotherm of V_2O_5–Al_2O_3 support.

3. Results and discussion

3.1 *Characterization*

The X-ray analysis of the V_2O_5–Al_2O_3 support (figure 1a) shows an amorphous structure. There is no significant indication for the presence of alumina or vanadium oxide. The X-ray pattern of the 5 wt% RuO_2/V_2O_5–Al_2O_3 catalyst (figure 1b) exhibits diffraction lines of the boehmite (JCPDS 21-1307) with well-defined peaks at $2\theta = 14°$, $28·5°$, $38·2°$, $49°$ and $66°$ which are assigned to (020), (120), (031), (051) and (231) planes, respectively (Reddy and Varma 2004; Amini *et al* 2005; Yang *et al* 2006). The peaks at $2\theta = 28°$ (110), $35°$ (101) and $54°$ (211) correspond to crystalline material with rutile phase, attributed to RuO_2 (Chen *et al*

2009; Jeng *et al* 2010; Matos *et al* 2010). Another peak at $2\theta = 44°$ (002) can also be seen and may be associated to the presence of metallic Ru (Manke *et al* 2005; Profeti *et al* 2006; Echeverri *et al* 2009). No peaks due to vanadium species were observed for the RuO_2/V_2O_5–Al_2O_3 sample, suggesting that vanadium was highly dispersed on the alumina surface or the crystallite size of the vanadium species was small that they were undetectable as a consequence of sensitivity and size limits of XRD technique (Yang *et al* 2006; Okal and Zawadzki 2007; Li *et al* 2009).

The nitrogen adsorption/desorption isotherms of the V_2O_5–Al_2O_3 support and RuO_2/V_2O_5–Al_2O_3 catalyst are shown in figures 2 and 3, respectively. The samples displayed isotherms of type IV according to IUPAC classification (Gregg and Sing 1982). The V_2O_5–Al_2O_3 support shows a
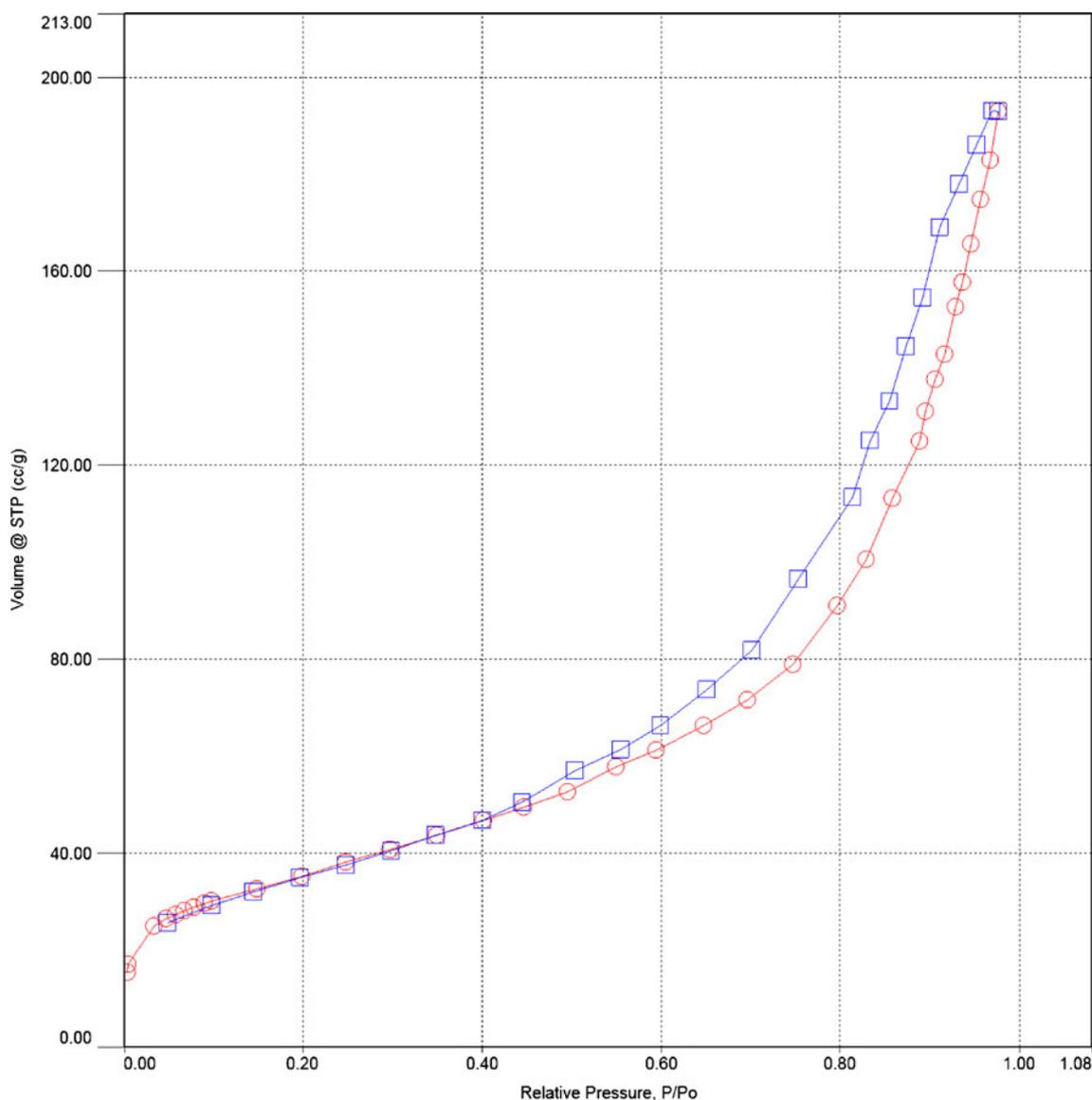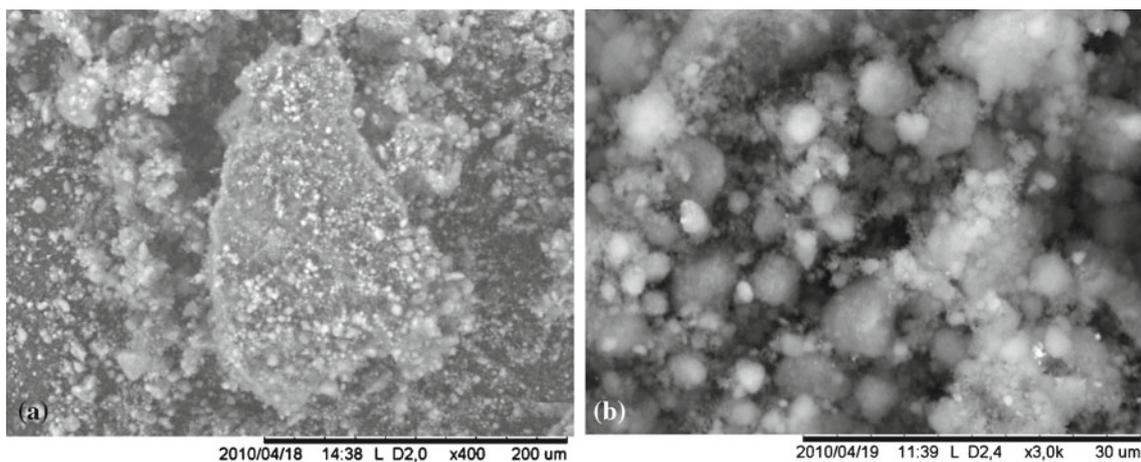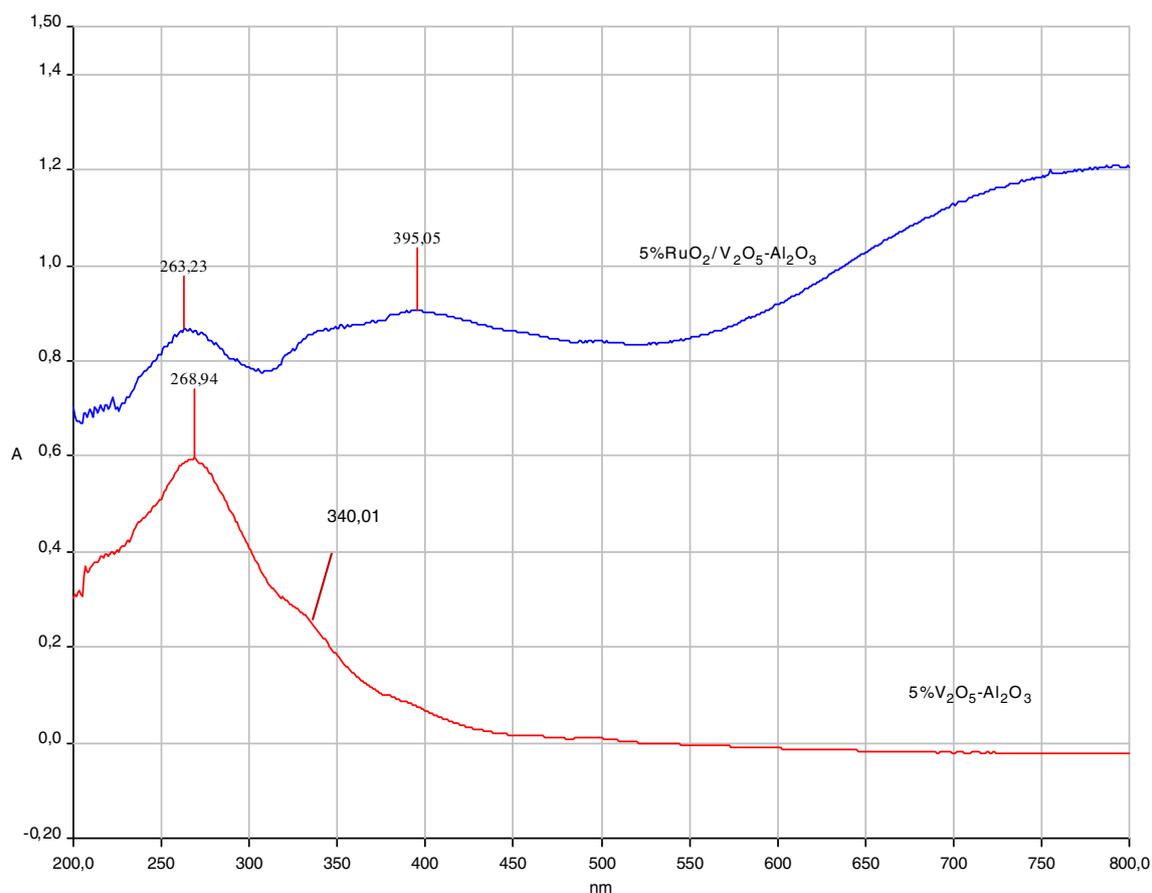

Figure 3. Nitrogen adsorption–desorption isotherm of RuO_2/V_2O_5–Al_2O_3 catalyst.

Table 1. BET surface area, pore volume and pore diameter.

Sample	BET surface area (m^2/g)	Pore volume (cm^3/g)	Pore diameter (nm)
$V_2O_5–Al_2O_3$	337·99	0·45	4·28
5 wt% $RuO_2/V_2O_5–Al_2O_3$	126·58	0·27	3·55

Figure 4. SEM images of $V_2O_5–Al_2O_3$ and $RuO_2/V_2O_5–Al_2O_3$ materials.

Figure 5. DR-UV-Visible spectra of $V_2O_5–Al_2O_3$ and $RuO_2/V_2O_5–Al_2O_3$ materials.

small hysteresis loop while the $RuO_2/V_2O_5-Al_2O_3$ catalyst presents a large hysteresis loop of type H1. These results are characteristics of mesoporous solids.

Quantitative comparisons on the pore structure of the $V_2O_5-Al_2O_3$ support and $RuO_2/V_2O_5-Al_2O_3$ catalyst are reported in table 1. The presence of RuO_2 had a great influence on the textural properties. The reduction in BET surface area, pore volume and pore diameter was presumably the result of blockage of some pores of $V_2O_5-Al_2O_3$ support by RuO_2 particles (Miller and Lakshmi 2000; Wang *et al* 2008).
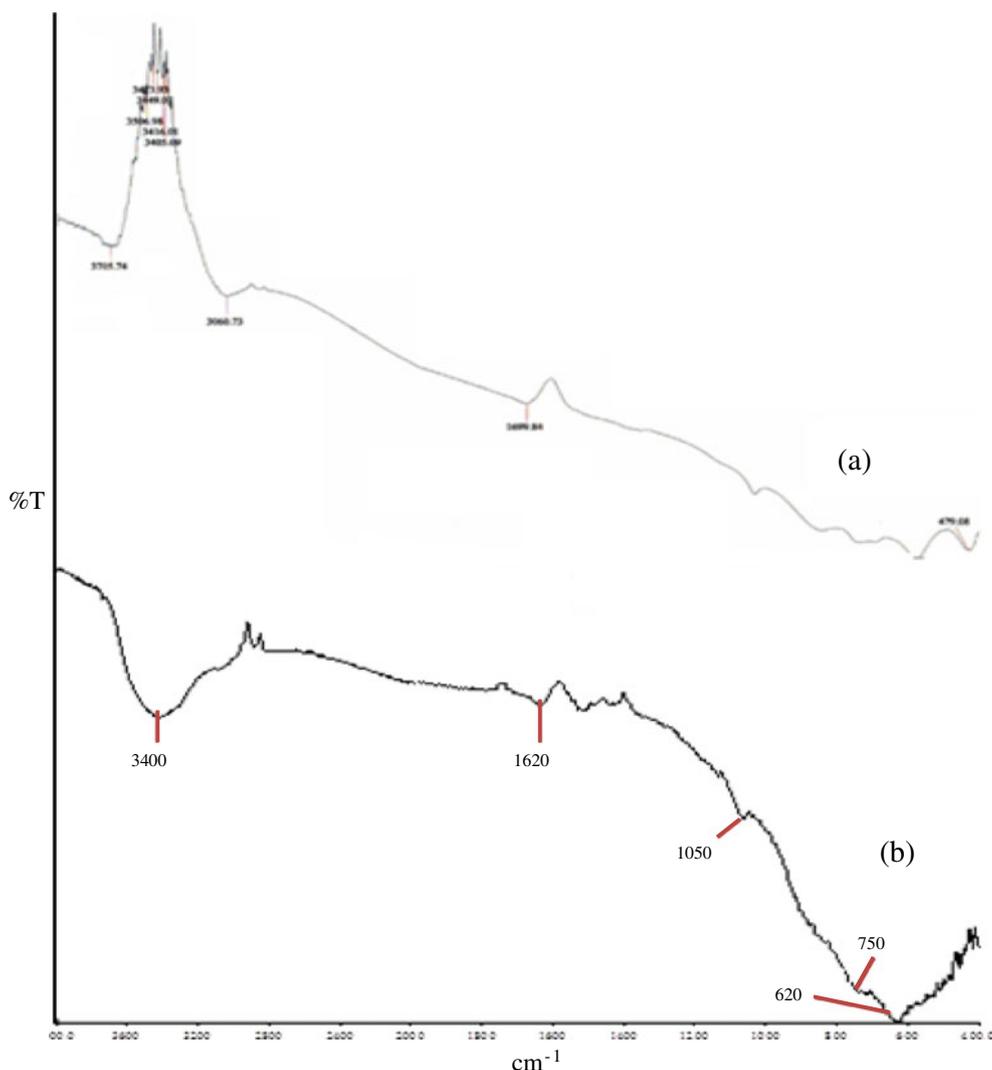

Figure 6. FT-IR spectra of $V_2O_5-Al_2O_3$ (a) and $RuO_2/V_2O_5-Al_2O_3$ (b) materials.

Table 2. Oxidation of cyclohexane with H_2O_2 catalysed by $RuO_2/V_2O_5-Al_2O_3$.

Solvent	Conversion (%)	Selectivity (%)		H_2O_2 consumption (%)
		Cy–OH	Cy=O	
None	0·00	0·00	0·00	92·54
Acetone	0·21	100	0·00	92·00
Acetic acid	4·40	22·18	77·82	77·61

Note: Cy–OH= cyclohexanol, Cy=O= cyclohexanone.
Reaction conditions: 66·5 m.mol cyclohexane; 66·5 m.mol H_2O_2; 24·8 ml solvent; 0·1 g $RuO_2/V_2O_5-Al_2O_3$ catalyst; $T = 343$ K; $t = 6$ h.

In figure 4, the SEM images of V$_2$O$_5$–Al$_2$O$_3$ and RuO$_2$/V$_2$O$_5$–Al$_2$O$_3$ materials are shown. For the support (figure 4a), we observe a cluster of small particles and absence of well-crystallized grains. This agrees with the XRD result which showed an amorphous structure of the V$_2$O$_5$–Al$_2$O$_3$ mixed oxide. Quite uniform and tiny particles almost spherical in shape were observed for RuO$_2$/V$_2$O$_5$–Al$_2$O$_3$ catalyst (figure 4b).

The diffuse reflectance UV-Visible spectra of V$_2$O$_5$–Al$_2$O$_3$ support and RuO$_2$/V$_2$O$_5$–Al$_2$O$_3$ catalyst (figure 5) exhibit bands around 265 nm characteristic of *d–d* transition of Al^{3+} ions. The spectrum observed for V$_2$O$_5$–Al$_2$O$_3$ exhibits a small band at 340 nm attributed to the charge transfer band associated with O^{2-} to V^{5+} in tetrahedral environment (Dapurkar *et al* 2004; Chen *et al* 2008; Aboelfetoh and Pietschnig 2009). Compared with V$_2$O$_5$–Al$_2$O$_3$ spectrum, we note an increase of intensity for RuO$_2$/V$_2$O$_5$–Al$_2$O$_3$ and apparition of a broad band around 395 nm which is probably due to the presence of ruthenium dioxide (Gao *et al* 2006).

Figure 6 shows IR spectra of the V$_2$O$_5$–Al$_2$O$_3$ support and RuO$_2$/V$_2$O$_5$–Al$_2$O$_3$ catalyst. The IR band at 3705·74 cm^{-1} (figure 6a) can be attributed to V–OH vibrations (Miller and Lakshmi 2000) and the band at 3060·73 cm^{-1} is due to OH stretching mode of hydroxyl groups, both from the interlayer water molecules and from Al–OH groups (Musić *et al* 2004; Ricci *et al* 2010). The deformation band of H$_2$O is situated at 1699·84 cm^{-1}. It was suggested that the band at 1080 cm^{-1} was due to Al–O–H bending vibrations of bridged hydroxyl groups on the surface of support (Reddy and Varma 2004). The band at 900–800 cm^{-1} is attributed to coupled vibration between V=O and V–O–V (Aboelfetoh and Pietschnig 2009). The band of the V–O bond is situated at 700–600 cm^{-1} (Bellifa *et al* 2006). At 480 cm^{-1}, we found the Al–O bending vibration band (Mirzaee *et al* 2005).

For the RuO$_2$/V$_2$O$_5$–Al$_2$O$_3$ catalyst (figure 6b), the wide band at 3400 cm^{-1} is characteristic of stretching vibration mode of –OH groups. In this work, presence of –OH groups can be assigned to H$_2$O molecules weakly adsorbed onto the surface of the material, and /or to Al–OH groups (AlO–H stretching) formed by hydrolysis of residual alkoxyde. The deformation band of H$_2$O is situated at 1620 cm^{-1}. The bands appearing between 1500 and 1400 cm^{-1} are attributed to the carbonate and carboxylate surface compounds formed

due to adsorption of atmospheric CO$_2$ on the supported material surface (Reddy and Varma 2004; Houšková *et al* 2009). The IR band at 1050 cm^{-1} is assigned to Al–O–H bending vibrations (Reddy and Varma 2004) and the band centred at 750 cm^{-1} can be due to Al–O stretching vibration (Mirzaee *et al* 2005; Ricci *et al* 2010). We designated the absorption band at 620 cm^{-1} as a Ru–O vibration mode (Jeng *et al* 2010).

3.2 *Catalytic tests*

As indicated by Almquist and Biswas (2001), effect of solvents on the oxidation rate of cyclohexane and on the alcohol to ketone ratio is significant. It was hypothesized that
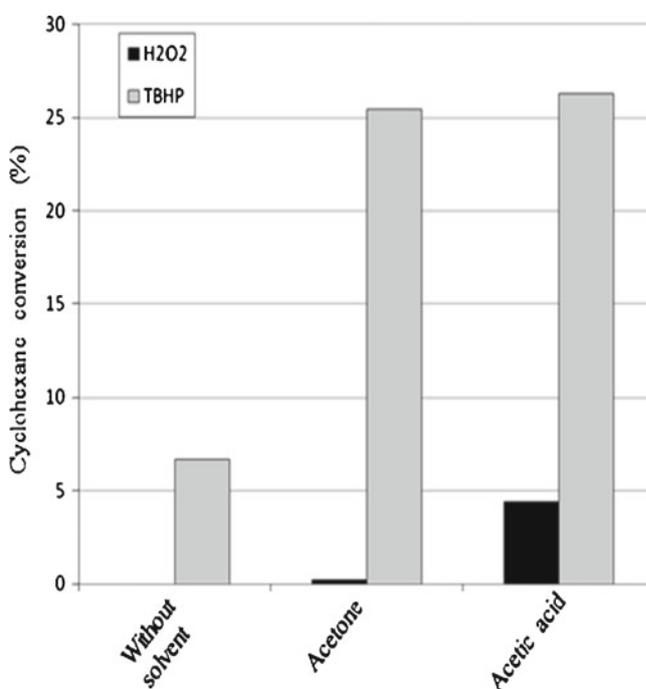

Figure 7. Effect of oxidant on cyclohexane conversion using RuO$_2$/V$_2$O$_5$–Al$_2$O$_3$ as catalyst in different solvents (66·5 m.mol cyclohexane; 66·5 m.mol oxidant; 24·8 ml solvent; 0·1 g catalyst; *T* = 343 K; *t* = 6 h).

Table 3. Oxidation of cyclohexane with TBHP catalysed by RuO$_2$/V$_2$O$_5$–Al$_2$O$_3$.

Solvent	Conversion (%)	Selectivity (%)		TBHP consumption (%)
		Cy–OH	Cy=O	
None	6·69	97·75	2·25	49·57
Acetone	25·45	76·66	23·34	52·17
Acetic acid	26·28	62·62	37·38	50·43

Note: Cy–OH= cyclohexanol, Cy=O= cyclohexanone.
Reaction conditions: 66·5 m.mol cyclohexane; 66·5 m.mol TBHP; 24·8 ml solvent; 0·1 g RuO$_2$/V$_2$O$_5$–Al$_2$O$_3$ catalyst; *T* = 343 K; *t* = 6 h.

the solvent changes the adsorption and desorption behaviour of cyclohexane and the corresponding oxygenates on the catalyst. In this work, we investigated the $RuO_2/V_2O_5–Al_2O_3$ catalyst in cyclohexane oxidation reaction using H_2O_2 or TBHP as oxidant; in acetone or acetic acid as solvent. The results are discussed below.

In order to disclose any solvent and oxidant effects on the reaction, we started with control tests (without catalyst). Whatever the oxidant used, no conversion was noticed after 6 h in absence of solvent. The addition of acetone or acetic acid did not produce any change, thus showing that the oxidation of C_6H_{12} remains a hard reaction.

The results of cyclohexane oxidation using $RuO_2/V_2O_5–Al_2O_3$ as catalyst and H_2O_2 as oxidant (table 2), did not show any conversion in absence of solvent; whereas a slight conversion percentage (0·21%) was found with acetone. The use of acetic acid as solvent produced better result with 4·4% conversion into cyclohexanol and cyclohexanone products.

However, in all cases studied, the consumption of H_2O_2 is more than 77% after 6 h of reaction. This effect may be due to
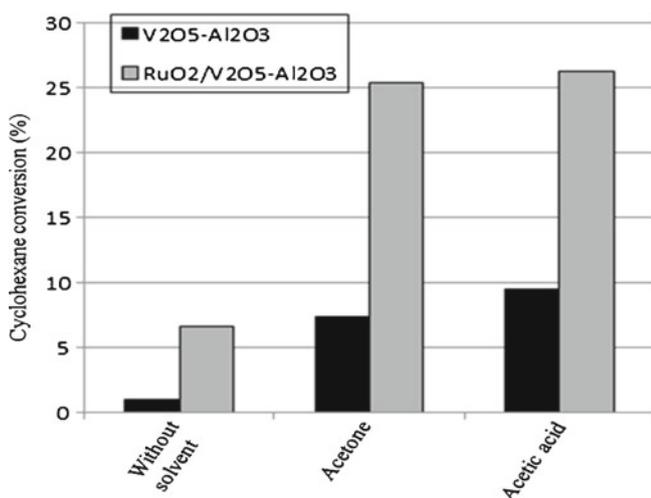

Figure 8. Effect of catalyst on cyclohexane conversion in different solvents (66·5 m.mol cyclohexane; 66·5 m.mol TBHP; 24·8 ml solvent; 0·1 g catalyst; $T = 343$ K; $t = 6$ h).

the liberation of uncomplexed V^{5+} or Ru^{4+}, which are prone to decompose H_2O_2 instead of reacting with cyclohexane (Aboelfetoh and Pietschnig 2009).

The catalytic activities of $RuO_2/V_2O_5–Al_2O_3$ material for the oxidation of cyclohexane with TBHP are represented in table 3. The catalyst has exhibited reasonably good activities and gives cyclohexanol as the predominant product. Approximately half of TBHP was consumed after 6 h of reaction.

These results are compared with those obtained with H_2O_2 as oxidant agent in figure 7. The cyclohexane conversions obtained by TBHP are much better. In acetic acid, we have approximately 6-fold higher conversion obtained with H_2O_2 (26·28% and 4·4%, respectively). This behaviour can be explained by the hydrophobicity relationship between the oxidant agent and the catalyst. To obtain a high activity of the catalyst for the liquid phase oxidation of alkanes, it is required that the hydrophobic substrate (e.g. cyclohexane) and the hydrophilic oxidant (e.g. TBHP) are adsorbed in equal amounts. Since H_2O_2 presents high hydrophilicity, it is probably retained preferentially on the outer surface of the $RuO_2/V_2O_5–Al_2O_3$ catalyst, not permeating into the channels and reaching the active sites which are located in the interior of the supported catalyst. Thus, its activation is limited to outer surface sites (Pires *et al* 2000).

The results of cyclohexane oxidation catalyzed by $RuO_2/V_2O_5–Al_2O_3$ material in TBHP as oxidant were also compared to those obtained with $V_2O_5–Al_2O_3$ support as catalyst in presence of TBHP (figure 8). It is very clear that RuO_2 supported on $V_2O_5–Al_2O_3$ catalyst gives the best conversions of cyclohexane.

For comparison purpose, cyclohexanol was submitted to reaction conditions in presence of H_2O_2 oxidant. It was already shown that the addition of cyclohexanol to the reaction mixture as initiator in the beginning of the reaction showed better results. On the other hand, addition of cyclohexanone to the reaction mixture lowered cyclohexane conversion (Cruz *et al* 2001, 2002; Pires *et al* 2001; Bellifa *et al* 2006).

The catalytic activities of $RuO_2/V_2O_5–Al_2O_3$ material for the oxidation of cyclohexane with H_2O_2 in presence of cyclohexanol as initiator are represented in table 4. A considerable

Table 4. Oxidation of cyclohexane with H_2O_2 in presence of cyclohexanol as initiator and catalysed by $RuO_2/V_2O_5–Al_2O_3$.

Solvent	Conversion (%)	Selectivity (%)		H_2O_2 consumption (%)
		Cy–OH	Cy=O	
None	11·12	99·86	0·14	86·60
Acetone	15·15	97·22	2·78	83·58
Acetic acid	40·10	92·27	7·73	88·81

Note: Cy–OH= cyclohexanol, Cy=O= cyclohexanone.
Reaction conditions: 66·5 m.mol cyclohexane; 66·5 m.mol H_2O_2; 19 mmol cyclohexanol; 24·8 ml solvent; 0·1 g $RuO_2/V_2O_5–Al_2O_3$ catalyst; $T = 343$ K; $t = 6$ h.

increase in cyclohexane conversions was observed. Using acetic acid as solvent, an approximately nine-fold increase in cyclohexane (40·10%) was noticed, compared to a system without initiator. The catalyst gives cyclohexanol as the predominant product with a selectivity more than 92%.

For all reactions with H_2O_2 or TBHP carried out with and without solvent, cyclohexane conversions increase in the order: without solvent < acetone < acetic acid. The presence of solvent makes the catalyst more active. Efficient removal of the oxidation products from the actives sites of the catalyst by the polar solvent is assumed to explain this weak activity (Pires *et al* 2001).

4. Conclusions

This work demonstrated the successful preparation of 5 wt% $RuO_2/V_2O_5–Al_2O_3$ catalyst by impregnation method. Texturally, the prepared material is formed by mesopores and presents a specific surface area of about 126·58 m^2/g. XRD, FT–IR and UV-visible analysis showed the presence of boehmite and RuO_2 with rutile variety. The V_2O_5 phase has not been observed.

The catalyst was found to be very effective for the liquid-phase oxidation of cyclohexane with tert-butyl hydroperoxide. However, it showed low conversions using hydrogen peroxide as oxidant. This behaviour has been explained by the hydrophobicity relationship between the oxidant agent and the catalyst. Best results are obtained in presence of cyclohexanol as initiator with hydrogen peroxide. In this reaction test, the conversion of cyclohexane to cyclohexanol and cyclohexanone and the selectivity ratio of cyclohexanol to cyclohexnone were greatly affected by the solvent and good yields were found in polar solvents. The use of acetic acid as solvent, cyclohexanol as initiator and H_2O_2 as oxidant presented an approximate 40% conversion with more than 92% selectivity for cyclohexanol product.

References

Aboelfetoh E F and Pietschnig R 2009 *Catal. Lett.* **127** 83

Almquist C B and Biswas P 2001 *Appl. Catal. A: Gen.* **214** 259

Amini M M, Sabounchei S J S, Mirnajafi F, Mirzaee M and Sharbatdaran M 2005 *Ceramics-silikáty.* **49** 138

Baccam N, Andrade J C, Godinho O E S and Barone J S 1985 *Quimica analytica quantitativa elementar* (Sao Paulo: Edgar Blucher Ltd.) 2nd ed., p. 201

Barrett E P, Joyner L G and Halenda P H 1951 *J. Am. Chem. Soc.* **73** 373

Bellifa A, Lahcene D, Tchenar Y N, Choukchou-Braham A, Bachir R, Bedrane S and Kappenstein C 2006 *Appl. Catal. A: Gen.* **305** 1

Brunauer S, Emmet P H and Taller E 1938 *J. Am. Soc.* **60** 309

Chęciński M P, Brückner A, Radnik J and Köckritz A 2009 *Appl. Catal. A: Gen.* **366** 212

Chen C A, Chen Y M, Chen K Y, Chi J K, Huang Y S and Tsai D S 2009 *J. Aloys & Compd* **485** 524

Chen F, Wu T H and Zhou X P 2008 *Catal. Commun.* **9** 1698

Cruz R S da, Silva J M S and Arnold U 2001 *J. Mol. Catal. A: Chem.* **171** 251

Cruz R S da, Silva J M S, Arnold U, Sercheli M S and Schuchardt U 2002 *J. Braz. Chem. Soc.* **13** 170

Dapurkar S E, Sakthivel A and Selvam P 2004 *J. Mol. Catal. A: Chem.* **223** 241

Echeverri D A, Marín J M, Restrepo G M and Rios L A 2009 *Appl. Catal. A: Gen.* **366** 342

Gao L B, Liu S H, Zhang L Y, Shi L X and Chen Z N 2006 *Organometallics* **25** 506

Ghiaci M, Aghabarari B, Do Rego A M B, Ferraria A M and Habibollahi S 2011 *Appl. Catal. A: Gen.* **393** 225

Gregg S J and Sing K S W 1982 *Adsorption surface area and porosity* (London: Academic Press) Ch. 1 & 6

Houšková V, Štengl V, Bakardjieva S, Murafa N and Tyrpekl V 2009 *Appl. Catal. B: Envir.* **89** 613

Jeng J S, Lin Y T and Chen J S 2010 *Thin Solid Films* **518** 5416

Lahcene D, Tchenar Y N, Choukchou-Braham A and Bachir R 2009 *Phys. Chem. News* **45** 121

Li Z, An X, Ren P, Huang W and Xie K 2009 *J. Nat. Gaz. Chem.* **18** 379

Mahmudov K T, Kopylovich M N, da Silva M F C G, Figiel P J, Karabach Y Y and Pombeiro A J L 2010 *J. Mol. Catal. A: Chem.* **318** 44

Manke C, Miedl S, Boissiere O, Baumann P K, Lindner J, Schumacher M, Brodyanski A and Scheib M 2005 *Microelectron. Eng.* **82** 242

Matos J, Rosale M, Cakan D and Titirici M M 2010 *Appl. Catal. A: Gen.* **386** 140

Miller J M and Lakshmi L J 2000 *Appl. Catal.* **190** 197

Mirzaee M, Amini M M, Sadeghi M, Mousavi F Y and Sharbatddaran M 2005 *Ceramics-Silikáty.* **49** 40

Musić S, Popocić S, Maljković M and Šarić A 2004 *Mater. Lett.* **58** 1431

Nada A A, Hamed H A, Barakat M H, Mohamed N R and Veziroglu T N 2008 *Int. J. Hydrogen Energ.* **32** 3264

Okal J and Zawadzki M 2007 *Appl. Catal. A: Gen.* **319** 202

Patake V D, Pawar S M, Shinde V R, Gujar T P and Lokhande C D 2010 *Curr. Appl. Phys.* **10** 99

Pires E L, Arnold U and Schuchardt U 2001 *J. Mol. Catal. A: Chem.* **169** 157

Pires E L, Magalhaes J C and Schuchardt U 2000 *Appl. Catal. A: Gen.* **203** 231

Profeti L P R, Simões F C, Olivi P, Kokoh K B, Coutanceau C, Léger J-M and Lamy C 2006 *J. Power Sources* **158** 1195

Rard J A 1985 *Chem. Rev.* **85** 1

Reddy E P and Varma R S 2004 *J. Catal.* **221** 93

Ricci C P, Rocha Z N, Nakagaki S, Castro K A D F, Crotti A E M, Calefi P S, Nassar E J and Ciuffi K J 2010 *Appl. Catal. A: Gen.* **389** 147

Schuchardt U *et al* 2001 *Appl. Catal. A: Gen.* **211** 1

Stuchinskaya T L, Musawir M, Kozhevnikova E F and Kozhevnikov I V 2005 *J. Catal.* **231** 41

Tchenar Y N, Lahcene D, Bellifa A, Bachir R and Choukchou-Braham A 2006 *Algerian J. Adv. Mater.* **3** 143

Wang J Y, Zhao F Y, Liu R J and Hu Y Q 2008 *J. Mol. Catal. A: Chem.* **279** 153

Wong L M, Wang S J and Chim W K 2010 *Thin Solid Films* **518** 93

Yang X, Erickson L E, Hohn K L, Jeevanandam P and Klabunde K J 2006 *Ind. Eng. Chem. Res.* **45** 6169

Yu H, Zhang Y, Fu X, Peng F, Wang H and Yang J 2009 *Catal. Commun.* **10** 1752